Jour. Fac. Sci., Hokkaido Univ., Ser. VII (Geophysics), Vol. 7, No. 2, 185–226, 1982.

On the Studies of the Periodic Motions in a Lake (II)
Effect of the Lake Basin Shape on the Periodic Motion

Shigeyoshi Kodomari

Department of Geophysics, Faculty of Science, Hokkaido University, Sapporo 060, Japan

(Received October 30, 1981)

Abstract

The periodic motion in a lake, known as the seiche, is studied comparing the numerical calculation with the observation. Considering this motion systematically, the effect of the lake basin shape on the motion can quantitatively be evaluated.

The characteristics of the motion are numerically investigated, using the two-dimensional model with typical lake shapes which have flat floors to evaluate the shore effect and have uneven bottoms to evaluate the bathymetric effect. Based on the numerical calculations, obtained are general formulas to evaluate the effect of the lake basin shape on the period. Generally, the shoreline effect including existence of islands prolongs a uninodal seiche period than that calculated in the rectangular lake model, but the bottom topography effect shortens that than that calculated using the mean depth. Comparing the periods estimated by these formulas with the observed ones in natural lakes, the characteristics of the basin shape effect become evident systematically regarding the periodic motion of lake water.

The flow patterns accompanying the periodic motion are considered in various typical lake shapes. The small irregularity of the lake shore hardly affects the motion, while an island or a peninsula changes the flow direction. These lake basin effects became clear quantitatively regarding the flow pattern of lake water. Considering these results, when the period is obtained by the general formulas, the flow pattern will be determined using the same lake model as the estimation.

Affected by the lake basin shape and the Coriolis force, the position of the nodal line changes unsteadily with time. However, the changes occur in almost the same place, so the position of the nodal line can be determined by a general formula. The calculated results approximately agree with the observations and the experimental studies by the writer and other investigators.

Considering the deflecting force of the earth's rotation, the periodic motion is hardly affected the period and the flow pattern by it except very large lakes such as a few hundred kilometers in length. Therefore, the deflecting flow of lake water is mainly controlled by the lake basin shape.

As a result, it is concluded that the seiche in a lake is not such a simple reciprocating motion as having been to date treated for calculations, but is the

periodic motion with the complex flow pattern affected by the lake basin shape. In other words, it is necessary to consider the factors as having been to date neglected for investigating this motion. And the general formulas are successful to evaluate the effect of the lake basin shape for various instances.

1. Introduction

If, in a lake, water piles up at the one end of it, water mass will flow to restore to the former water level. The flow, however, will not lose its energy when the surface becomes the flat stage, but will continue pilling water at the other end. It will cause a new flow in the opposite direction of the former. Thus, the lake water moves periodically, when it sets going by such external forces as the wind, the barometric pressure, and the earthquake. A flow system in a lake constitutes a periodic motion of water level, and this period depends on the dimension of the lake. The stationary oscillations of water level are known as seiches. This phenomenon has been recognized since early times. Chrystal (1905b) drew up a list of books and memoirs dealing with the seiche, extending from 1755 to 1905. And the earlier studies were largely summarized by Hutchinson (1957).

Now, taking x and y horizontal axes such that x is directed towards the east, y is directed towards the north. Here, h denotes the depth below the mean water level at $z=0$, η denotes the displacement of water, and u and v denote respectively the x and the y components of the flow. Then the equation of continuity is

$$\frac{\partial(hu)}{\partial x}+\frac{\partial(hv)}{\partial y}+\frac{\partial \eta}{\partial t}=0\,. \tag{1}$$

The equations of motion are

$$\left.\begin{aligned}\frac{\partial u}{\partial t}+u\frac{\partial u}{\partial x}+v\frac{\partial u}{\partial y}&=fv-g\frac{\partial \eta}{\partial x}+\nu\frac{\partial^2 u}{\partial z^2}\\ \frac{\partial v}{\partial t}+u\frac{\partial v}{\partial x}+v\frac{\partial v}{\partial y}&=-fu-g\frac{\partial \eta}{\partial y}+\nu\frac{\partial^2 v}{\partial z^2}\,,\end{aligned}\right\} \tag{2}$$

where f is the parameter of deflecting force of the earth's rotation (Coriolis parameter), g is the acceleration of gravity, and ν is the eddy viscosity. In the simplest case, water flows in the x direction of a rectangular lake with constant depth, while the frictional force, the geostrophic froce, and the horizontal acceleration are neglected. The differential equations become

$$\frac{\partial u}{\partial t} = -g\frac{\partial \eta}{\partial x} \tag{3}$$

$$h\frac{\partial u}{\partial x} = -\frac{\partial \eta}{\partial t}\,. \tag{4}$$

The ends of the lake are given by $x=0$ and $x=L$.

The flow velocity is put in the following,

$$u = C\sin\frac{\pi x}{L}\sin\frac{2\pi t}{T_1}\,, \tag{5}$$

where C is the constant speed, and T_1 is a period. This equation satisfies the conditions of $u=0$ at $x=0$ and $x=L$. On substituting the equation (5) into the equation (4), and integrated,

$$\eta = \frac{T_1 h}{2L}C\cos\frac{\pi x}{L}\cos\frac{2\pi t}{T_1}\,. \tag{6}$$

It follows from the equations (3), (5), and (6) that

$$T_1 = \frac{2L}{\sqrt{gh}}\,, \tag{7}$$

which is known as "Merian's formula" for a uninodal seiche. Although the basin of a natural lake largely deviates from the rectangular form, the period calculated by Merian's formula, using the lake length for L and the mean depth for h, approximately agrees with the observed one.

Many investigators have more elaborately treated the seiches in various cross sections of lake basins (e.g. Chrystal, 1904, 1905a, 1905b; Terada, 1906; Proudman, 1915; Defant, 1918; Jeffreys, 1925; Lamb, 1932; Hidaka, 1932a, 1932b, 1936, 1937; Ertel, 1933; Tuboi, 1936; Neumann, 1944a, 1944b; Clarke, 1971), some of them were summarized by Defant (1961), but most of their treatments were limited to one-dimensional methods or simple lake models such as a circular basin and a symmetric longitudinal section.

Until recently, many investigators have reported the seiches in various lakes using numerical calculations (e.g. Imasato, 1971, 1972; Platzman, 1972; Kanari, 1974; Kodomari, 1975, 1978; Hamblin, 1976; Rao and Schwab, 1976; Schwab and Rao, 1977). The useful information has been got through them, but their studies confined themselves to examine the periodic motion for particular lakes. The effect of the lake basin shape on this motion was not generally evaluated yet.

To investigate the motion, the period will be determined. The reason is because the period has much information about the motion, moreover, this can be observed more easily and exactly than the velocity of the flow. On the other hand, the amplitude of the seiche depends on the lake basin shape also on the energy that generates the motion, so the amplitude is very variable and is not suitable to investigate the motion.

When the numerical calculation was carried out in a natural lake, it confined itself to the particular lake. But various conditions and various lake models can easily be chosen to standarize the lake basin effect. For this reason, the numerical calculations have been performed, and general formulas for period have been sought. The results estimated by the general formulas have been compared with the periods obtained by observations, and the periodic motion has been considered according to those results.

In a previous paper (Kodomari, 1976), the island effect on the seiche period was investigated. The effect of the lake basin shape on the periodic motion will be investigated in this study.

2. Method

2.1 Procedure of the numerical calculation

Since the vertical acceleration is negligibly small compared with the horizontal one, the one-layer model is used in this study. The Coriolis force is taken into consideration. The bottom stress and the inertia terms which will affect the motion in shallow areas of a lake are incorporated into the equations of motion.

Integrating the equations of (1) and (2), the equations of continuity and motion become as follows:

$$\frac{\partial \eta}{\partial t} = -\frac{\partial Q_x}{\partial x} - \frac{\partial Q_y}{\partial y} \tag{8}$$

$$\left.\begin{aligned} \frac{\partial Q_x}{\partial t} &= -g(h+\eta)\frac{\partial \eta}{\partial x} + A_x \\ \frac{\partial Q_y}{\partial t} &= -g(h+\eta)\frac{\partial \eta}{\partial y} + A_y \,, \end{aligned}\right\} \tag{9}$$

Q_x and Q_y are the quantities defined by the equations

$$Q_x = \int_{-\eta}^{h} u\,dz = (h+\eta)\,u \tag{10}$$

$$Q_y = \int_{-\eta}^{h} v\,dz = (h+\eta)\,v\,, \tag{11}$$

and

$$A_x = \frac{\tau_{sx}}{\rho_w} - \frac{\tau_{bx}}{\rho_w} + fQ_y - (h+\eta)\left(\frac{\partial u^2}{\partial x} + \frac{\partial uv}{\partial y}\right) \tag{12}$$

$$A_y = \frac{\tau_{sy}}{\rho_w} - \frac{\tau_{by}}{\rho_w} - fQ_x - (h+\eta)\left(\frac{\partial uv}{\partial x} + \frac{\partial v^2}{\partial y}\right), \tag{13}$$

where τ_s is the wind stress at the water surface, τ_b is the bottom stress, and ρ_w is the density of water (1.0 g/cm^3). The surface wind stress is given by the equation

$$\tau_s = \rho_a\,\gamma_a{}^2\,\boldsymbol{W}\,|\,\boldsymbol{W}|\,,$$

where ρ_a is the density of air (0.0012 g/cm^3), $\boldsymbol{W}$ is the wind speed over the water surface, and $\gamma_a{}^2$ is the drag coefficient of air. $\gamma_a{}^2$ was given in this calculation the same value of 0.0013 after Imasato (1971). Hence, the equation becomes in the following,

$$\tau_s = 1.56\times 10^{-6}\,\boldsymbol{W}\,|\,\boldsymbol{W}|\,. \tag{14}$$

The bottom stress is written according to Imasato (1971),

$$\tau_b = 2.6\times 10^{-3}\,\boldsymbol{V}\,|\,\boldsymbol{V}\,| - \tau_s\,, \tag{15}$$

where $\boldsymbol{V}$ is the velocity vector of water.

Carried out the calculation, the wind field over the lake is adopted such a simple model as the wind blows uniformly (7 m/sec) during 20 minutes in the direction of the longitudinal lake axis. The initial condition is that the lake is at rest, namely, $\eta=u=v=0$ everywhere. The normal components of the velocity are zero at the shoreline as the boundary condition. The derivatives in the equations (8)–(13) have been replaced with the central differences individually.

To determine the seiche period, the spectrum of η is calculated by Fourier transform of the calculated time series ranged from 300 to 1000 minutes of duration in each lake model.

2.2 Application of the numerical calculations to natural lakes

Before the calculations were carried out in lake models, they were done in some natural lake models to estimate the effect of the lake basin shape on the seiche period. The uninodal seiche is exclusively examined in each lake.

The periodic motion in Lake Suwa, Nagano Prefecture in Japan, was calculated about four cases shown in Fig. 1. In these cases, a mesh interval is 500 m and a time interval is 5 seconds. The observed period is 20.8 min (Tanaka, 1911). The calculated periods are arranged around the observed one from 20.7 min in the case of the smallest lake area approximation (S–3) to 24.2 min in that of the largest lake area (S–1).

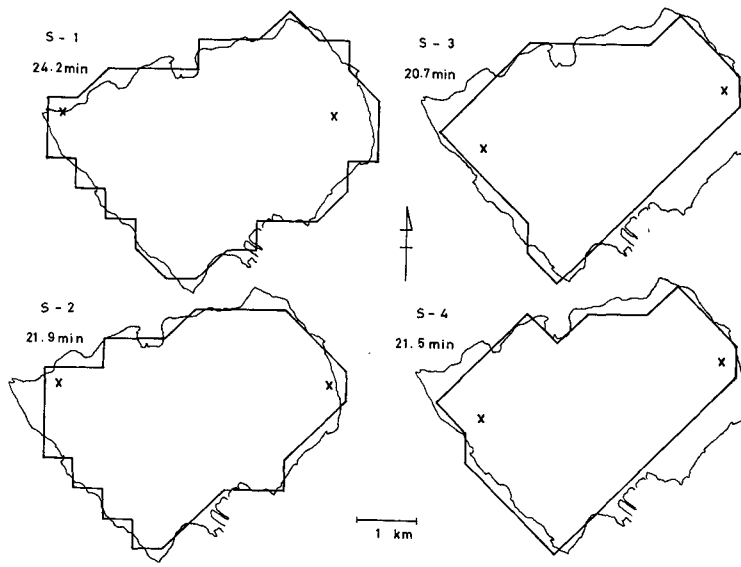

Fig. 1 Calculated areas of Lake Suwa. Calculated period (at point ×) is shown under the case number.

Fig. 2 shows the cases of Lake Yamanaka, Yamanashi Prefecture in Japan. A mesh interval is 250 m and a time interval is 2 seconds in these cases. In this lake, the observed period is 15.61 min (Nakamura and Honda, 1911). The calculated results show that the north-eastern part of the lake has the effect considerably on the seiche period, and this effect may not be shown in a rectangular model of Lake Yamanaka.

The lake has three basins in the southern part of Lake Towada, Aomori

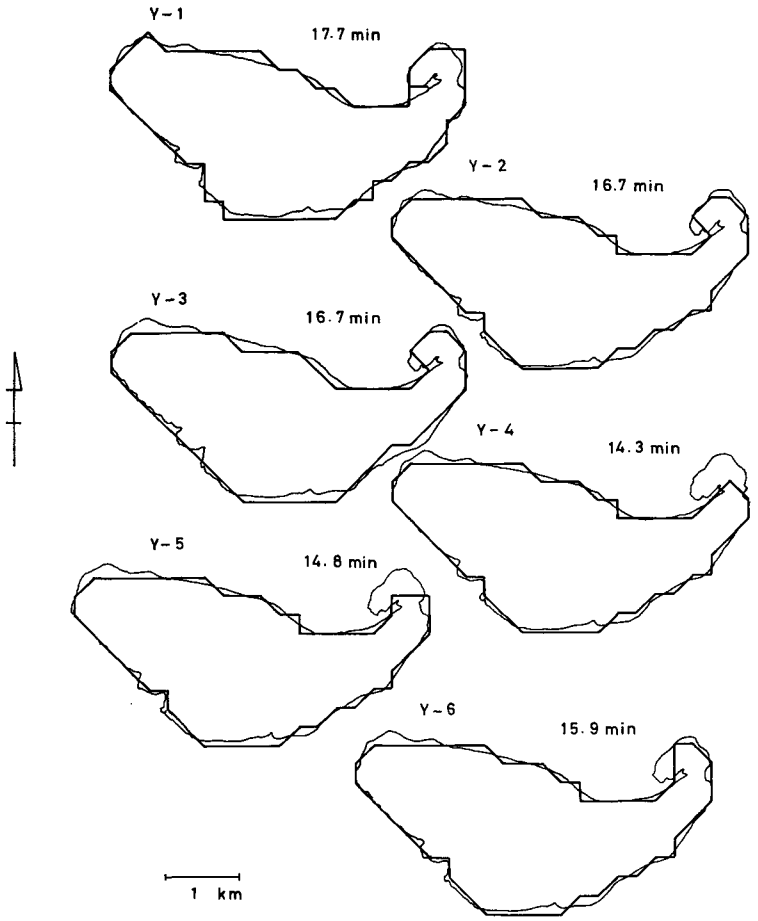

Fig. 2 Calculated areas of Lake Yamanaka. Calculated period is shown over the each lake model.

Prefecture in Japan, as shown in Fig. 3. The numerical calculations were carried out about two cases with a mesh interval of 1 km and a time interval of 5 seconds. The one (Tw–1) was calculated with all the effects of three basins, and the other (Tw–2) was done being neglected the effect of Naka-no-umi (middle of the three basins). The seiche is calculated as the period of 17.4 min in the case of Tw–1 and 17.5 min in Tw–2. These values agree well with the observation of 17.33 min (Honda et al., 1913). Accordingly, it is concluded that the effect of Naka-no-umi on the uninodal seiche is negligibly small.

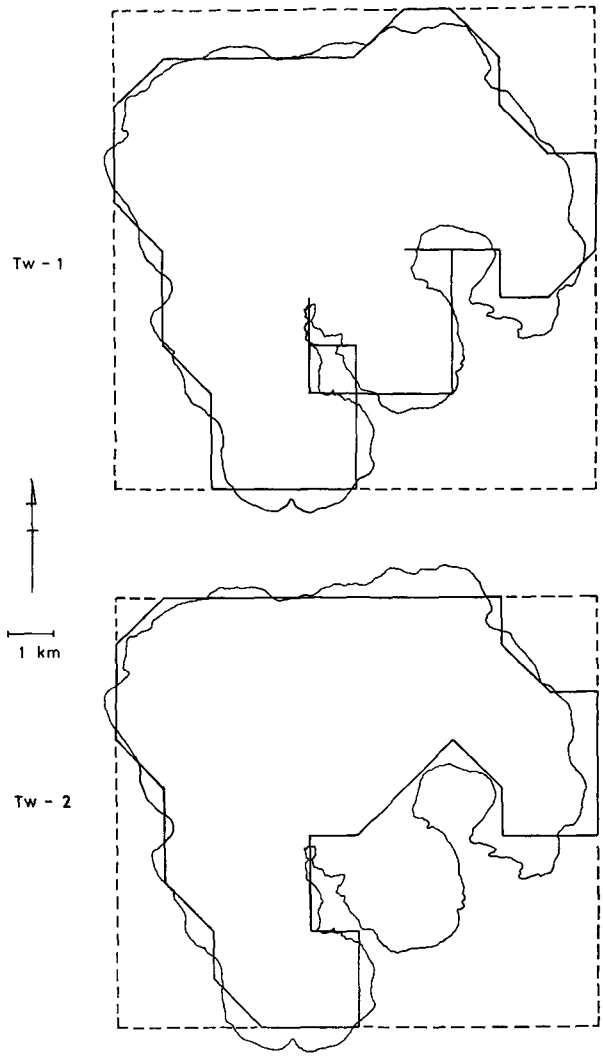

Fig. 3 Calculated areas of Lake Towada.

In Lake Toya, Hokkaido in Japan, the periods of 11.6 and 9.8 min were previously obtained by the numerical calculation with a mesh interval of 1 km, while the observed periods were 11.0 and 9.0 min (Kodomari, 1978). On a mesh interval of 500 m, the calculated periods are 11.1 and 9.1 min. Those agree better with the observed ones than the case of 1 km mesh interval. On the other hand, the different mesh intervals (500 m and 1 km) gave the same

calculated period of the longitudinal seiche in Lake Kutcharo, Hokkaido in Japan (Kodomari, 1975). This result, such that the calculated period with a certain mesh interval sometimes differs from the value with a different mesh interval, is probably attributed to the lake bottom topography. Namely, when the lake depth suddenly changes in comparison with a mesh interval, the calculated period may not indicate the suitable value. The fact of the difference between calculated periods with various mesh intervals has tendency to be happened in such a lake that the depth suddenly changes near the lake shore region.

In the numerical calculations, the seiche periods were changed with given lake models. Namely, the way of approximations of the shoreline and the lake bottom influences the seiche period. Therefore, it must be estimated the effect of the lake basin shape on the seiche period.

3. Numerical calculations in lake models and the general formulas for the seiche period

The numerical calculations have been carried out in various lake models. Table 1 shows the models of lakes. X indicates the longitudinal lake length, Y is the transverse one, and Δx is a mesh interval. Time interval is 5 seconds in the models of M–13 and M–14, and it is 10 seconds in the others. The Coriolis parameter is given as 0.0001/sec. When it is necessary to consider

Table 1 Models of lakes

Model	X (km)	Y (km)	Δx (km)
M-1	15	9	1
M-2	15	13	1
M-3	7	7	1
M-4	15	6	1
M-5	9	9	1
M-6	19	7	1
M-7	23	19	1
M-8	15	15	1
M-9	15	7	1
M-10	15	4	1
M-11	13	9	1
M-12	11	9	1
M-13	11.5	9.5	0.5
M-14	15.5	14.5	0.5

X; longitudinal lake length, Y; transverse lake length, Δx; mesh interval.

the particular cases of various conditions, other models are used in calculations to the comparison.

Firstly, the longitudinal uninodal seiche is examined.

3.1 Effect of the shoreline

To estimate the shoreline effect, the seiche periods were numerically calculated using typical lake models with complicated shorelines and constant depths of 10 m. These results were compared with the rectangular lake model (fundamental model) which had the same length and width as the complicated lake models. Some examples are shown in Fig. 4. The length of a projection (irregularity of the shoreline) in the direction of Y-axis is equivalent to a mesh interval of the model. When the shoreline effect is negligible small, T/T_0 is nearly equal to 1.0, and it becomes larger over 1.0 as the effect increases. As shown in this figure, when the ratio of Δx to Y is small (in the case M–14), the T/T_0 value of 1.02 does not change with $c \cdot S/S_0$. When the ratio is large (in the case M–1), T/T_0 changes with $c \cdot S/S_0$ and the period of a complicated model is more prolonged than the rectangular model.

From these results, it is concluded that the effect of the small irregularity in the lake shore can be neglected on the seiche period. Next, to estimate the effect of the large irregularity in the lake shore on the seiche period, the peninsula effect will be considered in typical lake models.

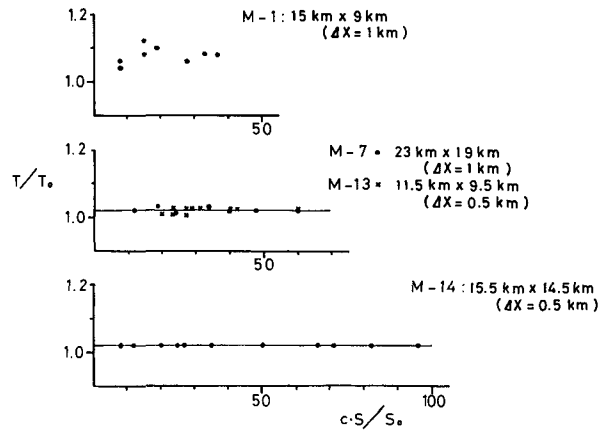

Fig. 4 Relation between the seiche period and the shoreline. T is a calculated period in the complicated lake model, T_0 is a period in a rectangular lake model, c shows the number of corners in the lake, S shows the area of the complicated lake model, and S_0 shows the area of the rectangular lake model.

3.2 *Effect of peninsulas*

Two various lake models, having a peninsula, are shown in Fig. 5. In these models, b and d indicate the longer distances between the peninsula and the lake shore in the X- and Y-directions respectively. The same relation about the periodic motion is also established in the contrary case ($b \leqq a$ or $c \geqq d$), because this motion moves back and forth in the lake.

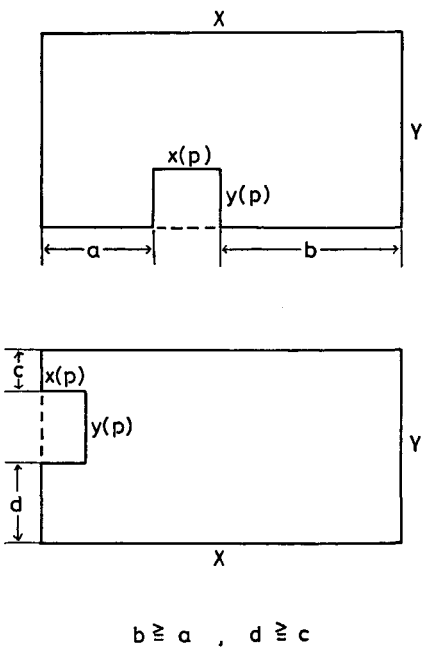

Fig. 5 Schematic models of the lake having a peninsula.

The relation between $x(p)$ and T/T_0 (in the model M–1) is shown in Fig. 6. The period has a maximum at a certain value of $x(p)$, and it increases with larger $y(p)$.

Subsequently, considered was the effect of the peninsula position on the period. Fig. 7 shows the relation between the position and the period (in the model M–1). The peninsula effect in the middle region of the lake is larger than that in the corner of the lake. Because the water mass can not easily move in such a narrow region between the lake shore and the peninsula near the corner of the lake, the peninsula effect near the corner becomes smaller

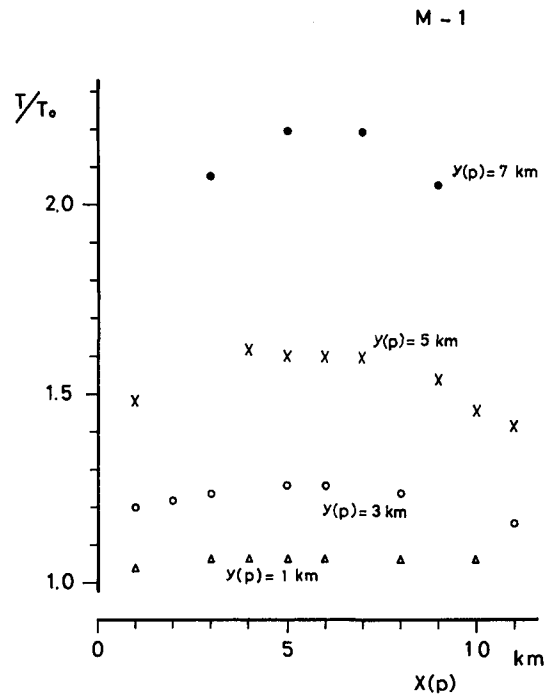

Fig. 6 Relation between the seiche period and the peninsula size (in the model M–1).

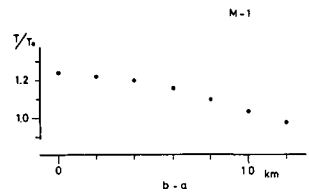

Fig. 7 Relation between the seiche period and the position of a peninsula (I). Both the length and the width of the peninsula are 3 km (in the model M–1).

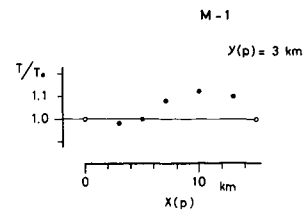

Fig. 8 Relation between the seiche period and the position of a peninsula (II). The peninsula exists at a corner in the lake model (in the model M–1).

than that in the middle region of the lake. When the peninsula is at a corner of a lake, the period changes more complicatedly. Fig. 8 shows an example in the model M–1. When $x(p)$ is small, the peninsula affects the periodic motion to shorten the lake length, so the period is shortened than a fundamental one. When $x(p)$ becomes larger, the water mass flows along this peninsula so that the period is more prolonged than the fundamental one. But, when $x(p)$ becomes larger still more, the water mass between the lake shore and the peninsula becomes hard to move, so the period gradually approaches the fundamental one.

From these facts stated above, considering the corelation by the each factor, general formulas are derived in the following. Non-dimensional variables are given as follows:

$$x_1 = x(p)/X\,, \qquad x_2 = y(p)/Y\,,$$
$$x_3 = Y/X\,,$$
$$x_4 = (b-a)/X\,, \qquad x_5 = c/(Y-y(p))\,,$$

where $y(p) \neq Y$. The variables of x_1 and x_2 are regarding the size of the peninsula, x_3 is the ratio of the transverse lake length to the longitudinal one, and the variables of x_4 and x_5 are regarding the position of the peninsula. Here T_c denotes the calculated period, the general formulas are given by

$$T_c = T_0\{1.0+P_1(1.0+Q_1)\} \tag{16}$$
(when $a \neq 0$ or $c \neq 0$)
$$= T_0\{1.0+P_1(1.0+Q_1)(1.0+Q_2)\} \tag{17}$$
(when $a=0$ and $c=0$),

where
$$T_0 = 2X/\sqrt{gh} \tag{18}$$
$$P_n = \Delta T/T_0 \qquad (n = 1, 2, 3) \tag{19}$$
$$Q_n = \Delta P/P_1 \qquad (n = 1, 2, 3, 4)\,, \tag{20}$$

and

$$P_1 = (x_1+x_2x_3)(1.0-x_1)/\{2(1.0-x_2)\}$$
$$Q_1 = -x_4{}^2-x_5$$
$$Q_2 = (x_1/x_3)-4(1.75-x_3)/3\,.$$

The equation (18) is equal to the equation (7). P_n is the ratio of a period increment (ΔT) to a fundamental period (T_0), Q_n is the correction term of P_1,

P_1 is the term on the peninsula size, and Q_1 and Q_2 are the correction terms on the position of the peninsula.

Fig. 9 shows the relation between the periods estimated by the general formulas and those obtained by the numerical calculations. The estimated values almost agree with the numerically calculated ones.

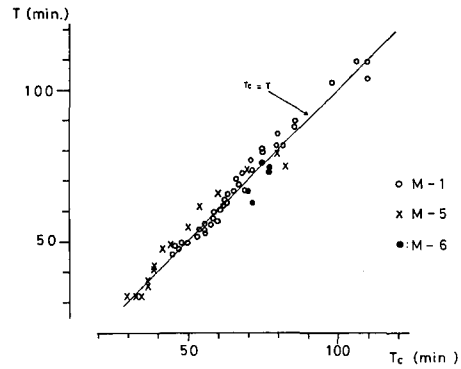

Fig. 9 Comparison between the period estimated by the general formulas (T_c) and that obtained by the numerical calculation (T).

In natural lakes, it is considered that the irregularity of the shoreline can be expressed as some peninsulas. Here, the numerical calculations are carried out with lake models in which there are two or three peninsulas. As a result of these calculations, it can be obtained the following conclusions. When two peninsulas exist close by each other, such that the length in the Y-direction of the larger one is longer than the distance between them, two peninsulas may be considered to be one peninsula which is equal in size to two peninsulas put together. When the one is extremely larger than the others, it is sufficient to consider only the larger one. When two peninsulas face each other in the Y-direction, the variables of x_2 and x_5 must differently be understood, that Y is replaced by Y' which is narrowed by the another peninsula. In other cases, it is considered that the effect of the peninsulas is expressed as the summation of every ones. Fig. 10 shows the results of estimations in lake models having plural peninsulas. The estimated values agree well with the numerically calculated ones. Therefore, the general formulas can be applied to lake models there are plural peninsulas in.

Peninsulas in natural lakes are not rectangular shapes. It is necessary to consider the varied shapes of peninsulas in the numerical calculations.

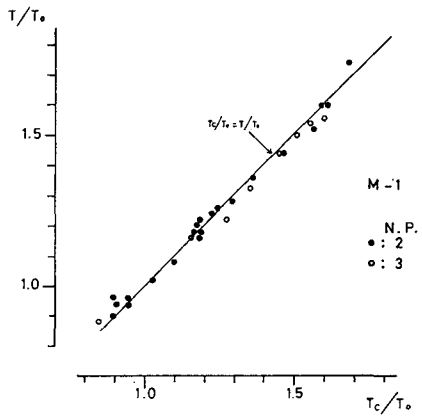

Fig. 10 Comparison between the period ratio estimated by the general formulas (T_c/T_0) and that obtained by the numerical calculation (T/T_0). In these lake models (in the model M–1), there are plural peninsulas. Solid circle shows the case of two peninsulas, and open circle shows that of three ones.

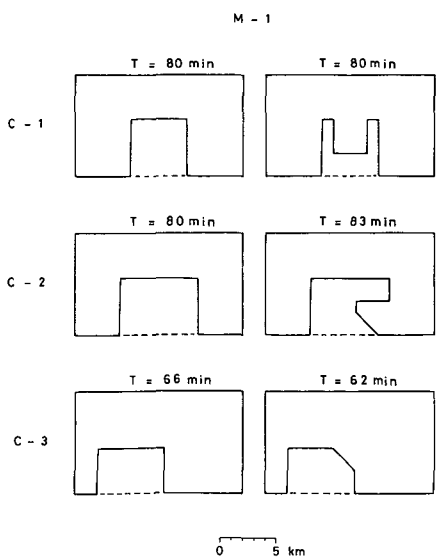

Fig. 11 Relation between the seiche period and the shape of the peninsula (I). T is a calculated period.

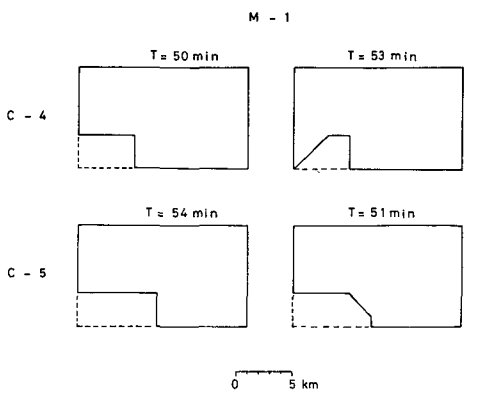

Fig. 12 Relation between the seiche period and the shape of the peninsula (II).

Some examples are shown in Figs. 11 and 12 (in the model M–1), in which the left side examples show the rectangular peninsulas and the right side ones show the more complex shapes. When a peninsula has a cove in the middle part of it (case C–1 in Fig. 11), the period does not vary the value which is calculated in the model with a rectangular peninsula. The physical meaning is considered that the water mass in the cove becomes dead water and stagnates during the motion, so there is no effect on the period. This phenomenon is seen in Lake Towada (shown in Fig. 3). The estimation in this case, therefore, can be made in the same way as the case of the rectangular peninsula. When a peninsula has a cove on the side of it (case C–2 in Fig. 11) or has a embayment at near the corner of a lake (case C–4 in Fig. 12), the period becomes longer than that in the rectangular peninsula model, because the reverse flow occurs in the cove or the embayment. In the case of cutting off the corner of a peninsula (cases C–3 in Fig. 11 and C–5 in Fig. 12), the period becomes shorter than that in the rectangular peninsula model. In this case, the lake water smoothly flows along that corner. For other special cases, the numerical calculations were also performed using various models in which there was a triangular peninsula at a corner of the lake. Fig. 13 shows the relation between the period ratio (T/T_0) and the length of a peninsula in the X-direction. The period variance, accompanying the length change of the triangular peninsulas, varies with each lake model. Generally, the effect of a triangular peninsula is smaller than that of the rectangular one, because the lake water smoothly flows along the oblique side of the peninsula.

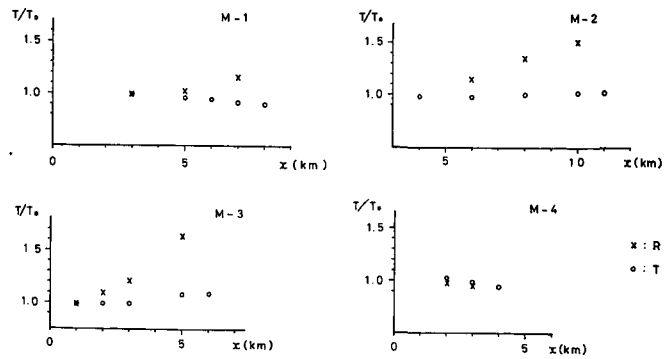

Fig. 13 Relation between the seiche period and the shape of the peninsula (III). Cross shows the case of a rectangular peninsula, open circle indicates that of a triangular one, and x is the length of the peninsula in the X-direction.

From the facts described above, the general formulas (16) and (17) are corrected as follows: The schematic lake model is changed as shown in Fig. 14. Following non-dimensional variables are obtained, using the new variables in this figure.

$$x_6 = B/A\,, \qquad x_7 = (D-C)/Y\,, \qquad x_8 = (A-B)/X\,,$$
$$x_9 = x(t)/X\,, \qquad x_{10} = y(t)/Y\,.$$

The variables regarding the peninsula shape are x_6, x_7, and x_8, the variables regarding the size of a triangular peninsula are x_9 and x_{10}. The correction terms affected by the peninsula shape are given in the following,

$$Q_3 = -(1.0-x_6)\,x_7\,,$$
$$P_2 = -x_7 x_8\,.$$

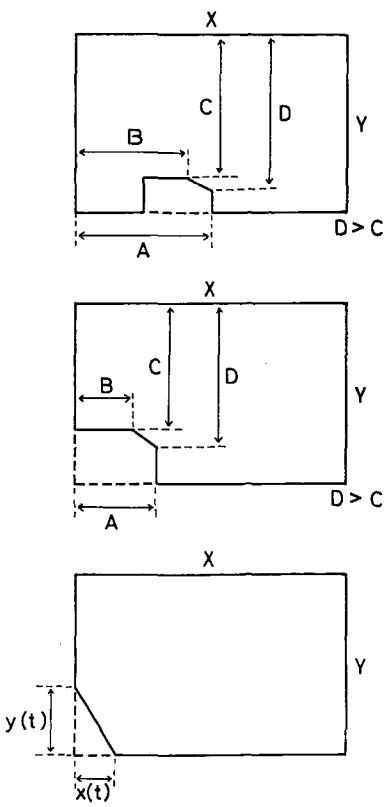

Fig. 14 Schematic models of the lake having an unsquared peninsula.

A term of P_3 in regard to the size of the triangular peninsula is indicated by the equation,

$$P_3 = (x_3x_9-0.5)\, x_9x_{10}-x_9^2(x_9-2x_3/3)\,.$$

The calculated period is given by

$$T_c = T_0\{1.0+P_1(1.0+Q_1)(1.0+Q_3)\} \tag{21}$$

(when $a\neq 0$ or $c\neq 0$)

$$= T_0\{1.0+P_1(1.0+Q_1)(1.0+Q_2)+P_2\} \tag{22}$$

(when $a=0$ and $c=0$)

$$= T_0(1.0+P_3) \tag{23}$$

(when $a=0$ and $c=0$, triangular peninsula).

Fig. 15 shows the relation between the value of T_c/T_0 and the value of T/T_0 calculated in the model M–1. The estimated periods coincide well with the numerically calculated ones.

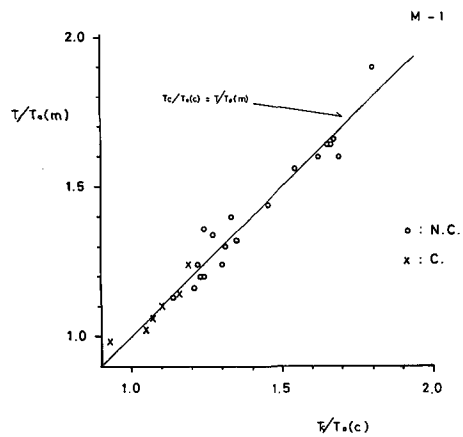

Fig. 15 Comparison between the period ratio estimated by the general formulas (T_c/T_0 (c)) and that obtained by the numerical calculation (T/T_0 (m)) (in the model M–1). Cross shows the case of a peninsula existing at a corner, and open circle shows that in other position.

The periods in natural lakes are estimated by the general formulas, and the results are shown in Fig. 16. The ordinate is the ratio of an observed period (T_{obs}) to a fundamental one (T_0), and the abscissa is an estimated value

using the general formulas (T_c/T_0(c)). The periods estimated by the general formulas differ consideringly from the observed ones, it is possibly because of the calculation using the mean depth regardless of the bottom topography. The bottom effect will be evaluated in the latter section.

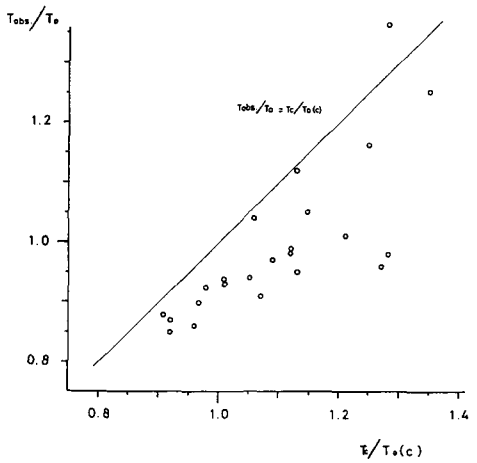

Fig. 16 Comparison between the period ratio estimated by the general formulas (T_c/T_0(c)) and that obtained by the observation (T_{obs}/T_0) in the natural lake.

3.3 Effect of islands

It is known that in a lake having an island the seiche period becomes longer than the case of no island (Kodomari, 1975, 1976). In the previous paper (Kodomari, 1976), the general formulas had been obtained. They are rewritten using the non-dimensional variables in the preceding section.

Fig. 17 shows a schematic lake model having an island. The effect of the island shape on the seiche period is formularized in the same form as the equations P_1 and Q_3 of the peninsula. The equation representative of the island location is slightly different from the equation Q_1 of the peninsula. Now, a non-dimensional variable of x_{11} regarding the island location is shown in the following,

$$x_{11} = (b-a)/(X-x(p)) \qquad \text{(where } X \neq x(p)\text{)},$$

and a correction term for the island location is given in the following,

$$Q_4 = -x_{11}^2 - x_5^2 x_3 .$$

Then, the equation of the period is

$$T_c = T_0\{1.0+P_1(1.0+Q_4)(1.0+Q_3)\} \quad (24)$$

(when $a \neq 0$ and $c \neq 0$).

This formula is the same form as the equation (9) in the previous paper (Kodomari, 1976), excluding the term of Q_3. The equation (24) is applied to natural lakes, and the estimated results are shown in Table 2. On comparing $(T/T_0)_{obs}$ with $(T/T_0)_{cal}$, there is respectable difference between them, because the fundamental period was calculated by Merian's formula assuming that the lake had a rectangular shape and a constant depth. Performed already in

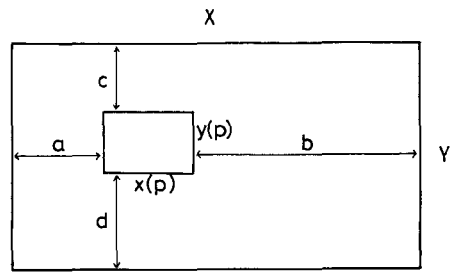

$b \geqq a$, $d \geqq c$

Fig. 17 Schematic model of the lake having an island.

Table 2 Comparison between the ratio of the observed period to the fundamental one and the period ratio estimated by the general formulas in the natural lake having islands.

Lake	T_{obs}(min)	T_0 (min)	Authors	$(T/T_0)_{obs}$	$(T/T_0)_{cal}$
Lake Baikal	278	270	Proudman (1953)	1.03	1.07
Biwa-ko	229.8	113**	Imasato et al. (1973)	2.03	1.04
Chiemsee	41	31.6**	Endrös (1906a)	1.30	1.07
Lake Erie	863	1008	Platzman and Rao (1964)	0.86	1.01
Kawaguchi-ko	22.98	20.1	Nakamura and Honda (1911)	1.14	1.06
Kutcharo-ko	30	25.8	Kodomari (1975)	1.16	1.17
Lake Lappajärvi	93	86	Simojoki (1961)	1.08	1.16
Lake Pyhäjärvi	101	116	Simojoki (1961)	0.87	1.02
Toya-ko	11.0	10.6**	Kodomari (1978)	1.04	1.20
Lake Vetter	178.99	203**	Bergsten (1926)	0.88	1.05
Lake Winnipeg	780*	774	Einarsson and Lowe (1968)	1.01	1.07

* Seiche in northern basin ** Calculated by Kodomari

the previous paper (Kodomari, 1976), on the calculations including the effect of the lake basin shape to a certain extent the differences were smaller than the present results in some lakes.

3.4 Effect of the bottom topography

In the preceding sections, the models were supposed with the constant depth of 10 m, and the periods in natural lakes were calculated using the mean depths. But the estimated periods were little coincident with the observed ones.

Though the mean depth is equal to each of all cases as shown in Fig. 18, the seiche periods are different from one another. For instance, when the values are used as 10 m, 20 m, and 7.5 km for h, h', and L respectively, the each period is 44, 38, and 41 min from the left to the right in this figure respectively. The physical meaning is considered that the period varies inversely as the velocity of the motion such as formularized in the equation (7), so the region being deeper than the mean depth affects the period to shorten it and the shallower region prolongs the period. Because the water in narrow deep can not easily come out, the narrow deep does not affect too much the periodic motion. The water on the shallower region except the longshore region moves with the periodic motion, so the shallower region considerably affects the seiche period. The seiche period is depended on these effects together.

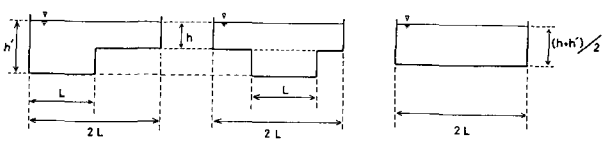

Fig. 18 Simple lake models having the same mean depth.

The numerical calculations were performed in various lake models with various bottom topographies, and a general formula was obtained taking note of the flat region of the lake floor such as the deep and the shallow possessing a certain extent. A schematic lake model is shown in Fig. 19. Non-dimensional variables are given as follows:

$$y_1 = x'/X\,, \qquad y_2 = y'/Y\,,$$
$$y_3 = Y/X\,,$$
$$y_4 = (b'-a')/X\,, \qquad y_5 = (d'-c')/Y\,.$$

The variables of y_1 and y_2 have regard to the size of the deep (or shallow), y_3 is the ratio of the transverse lake length to the longitudinal one, and the variables of y_4 and y_5 have regard to the location of the deep (or shallow).

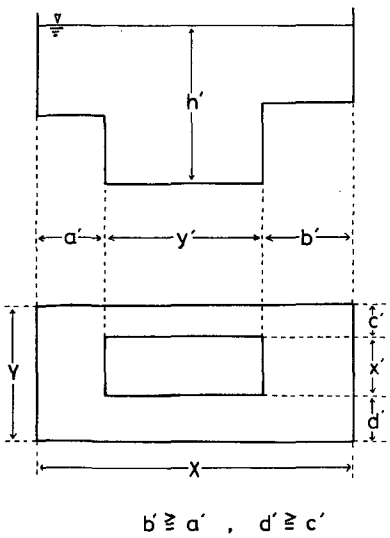

Fig. 19 Schematic model of the lake with uneven bottom floor.

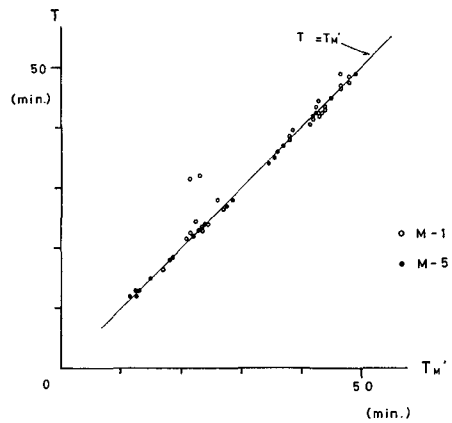

Fig. 20 Comparison between the period estimated by the general formula (T_M') and that obtained by the numerical calculation (T).

Indicating the mean depth with h_m and the depth of the deep (or shallow) with h', an increment of the depth (Δh) is given by

$$\Delta h = (h_m - h')\, y_1 y_2 (1.0 - y_3 y_4)(1.0 - y_5) ,$$

and the corrected depth (h^*) is given by

$$h^* = h_m - \Delta h .$$

Then the fundamental period is formularized in place of the equation (18) in the following,

$$T_M' = 2X / \sqrt{gh^*} . \tag{25}$$

Fig. 20 shows the relation between the period estimated by the equation (25) and that obtained by the numerical calculation using the model with uneven bottom floor. The close agreement between them is obtained.

Table 3 shows the corrected values for the mean depths in natural lakes. As a result, it is considered that the value of the mean depth requires 5~15%

Table 3 Corrected values of the depth in natural lakes

Lake	h_m (m)	$-\Delta h$ (m)	$\lvert\Delta h\rvert/h_m$
Ammersee	42.6	4.2	0.10
Aoki-ko	29.0	2.5	0.09
Ashi-no-ko	18.8	3.2	0.17
Lake Baikal	680	26	0.04
Lake Balaton	3.0	0.0	0.0
Biwa-ko	41.2	4.3	0.10
Lake Brienz	174	19	0.11
Chiemsee	24.5	−2.6	0.11
Chuzenji-ko	94.6	5.1	0.05
Lake Constance	100.0	2.5	0.03
Loch Earn	60.0	1.4	0.02
Lake Erie	18.2	0.0	0.0
Lago di Garda	136.1	18.5	0.14
Lake Geneva	152.7	4.7	0.03
Goldberger See	2.0	0.1	0.05
Great Bear Lake	75.4	1.8	0.02
Green Lake	33.1	4.6	0.14
Lake Huron	60	4	0.07
Inawashiro-ko	51.4	4.0	0.08
Kasumi-ga-ura	4.0	0.3	0.08
Kawaguchi-ko	9.8	0.1	0.01
Kizaki-ko	17.9	2.5	0.14
Kutcharo-ko	28.4	2.8	0.10
Kuttara-ko	105	10	0.10
Lake Lappajärvi	7.5	0.0	0.0
Madüsee	18.7	2.8	0.15
Lake Mendota	12.1	0.7	0.06
Lake Michigan	85.3	2.0	0.02
Lough Neagh	10.5	0.5	0.05
Loch Ness	133	16	0.12
Nojiri-ko	21.0	1.6	0.08
Lake Ontario	79	13	0.16
Lake Pyhäjärvi	5.5	0.0	0.0
Shikotsu-ko	256	31	0.12
Starnberger See	52	3.8	0.07
St. Wolfgang See	47.1	−3.7	0.08
Lake Superior	146	14	0.10
Suwa-ko	4.1	0.4	0.10
Lake Tahoe	313	32	0.10
Lake Tanganyika	572	127	0.22
Tazawa-ko	280.0	26.3	0.09
Towada-ko	56	4	0.07
Toya-ko	122	8	0.07
Loch Treig	63.2	8.0	0.13
Lake Vetter	38.9	4.0	0.10
Waginger-Tachinger-Sees	12.8	−0.7	0.05
(Waginger-See	15.0	1.4	0.09)
(Tachinger-See	9.6	0.2	0.02)
Lake Wakatipu	200	34	0.17
Yamanaka-ko	9.2	0.4	0.04

h_m; mean depth, Δh; increment of the depth

correction for calculating the seiche period. And the maximum value of the correction is 22% in Lake Tanganyika. In this table, the signs of the increment are reversed in three lakes. Extended about a quarter of whole basin of Chiemsee, the region which surrounds the islands is shallower than the mean depth of this lake, so the sign of the increment is reversed. In St. Wolfgang See and Waginger-Tachinger-Sees, because they consist of two basins connected by shallower channels, the effects of these channels reverse the signs of the increment. On the other hand, Lakes Balaton, Erie, Lappajärvi, and Pyhäjärvi have roughly flat lake floors being nearly equal to the mean depths, so the increment is zero in each lake.

The increment values are mostly negative in natural lakes as shown in Table 3, so that these corrections generally act to shorten on the seiche periods.

3.5 Application of the general formulas to natural lakes

The general formulas were used to estimate the seiche periods in natural lakes. Firstly, Lakes Kutcharo and Toya are used as examples. Fig. 21 shows three outlines of Lake Kutcharo. The rectangular model in the case of K–1 differs from that in the case of K–2 in the length and the width, and also differs in the shapes of the island and the peninsulas being surrounded by the broken and the solid lines, but two models have almost the same lake outline. On the other hand, the north-eastern cove in this lake is neglected in the case of K–3. The period in K–1 is estimated by the general formulas at 30.3 min the same as it in K–2 and it is 28.3 min in K–3, while the observed one is 30 min after Kodomari (1975). Therefore, it is concluded that the uninodal seiche is occurred over the whole basin in this lake.

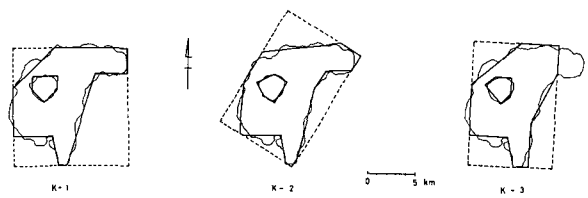

Fig. 21 Calculated areas of Lake Kutcharo.

In Lake Toya, the two predominant periods were observed as 11.0 and 9.0 min by Kodomari (1978). The former value is the period resulting from the flow in the E-W direction, and the latter is that in the N-S direction.

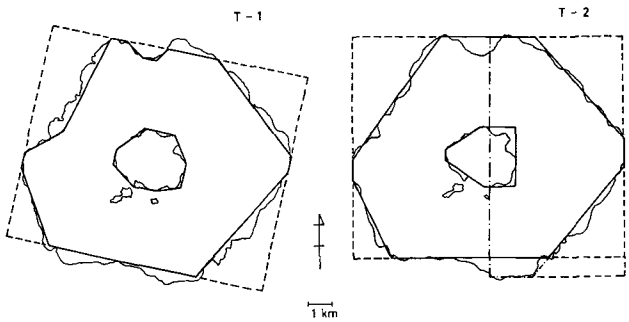

Fig. 22 Calculated areas of Lake Toya.

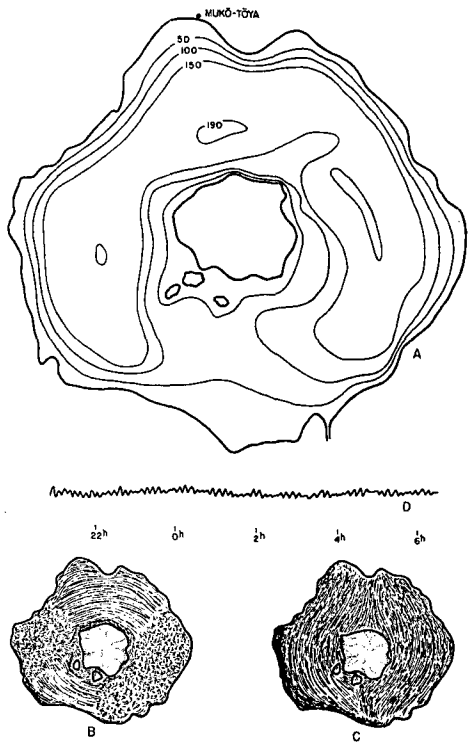

Fig. 23 Lake Toya. A: bathymetric map, B and C: vibration patterns of aluminum powder on the surface in a model, D: limnogram taken at Muko-Toya. (After Nakamura and Honda) (According to Hutchinson, 1957).

Supposing the case of E-W direction, the period is estimated at 11.2 min in the model of T–1 as shown in Fig. 22. In the model of T–2, the estimated period supposing the E-W direction is 11.2 min and the same as that in T–1. A similar value of 11.3 min is estimated supposing the N-S direction in the model of T–2. Lake Toya has a nearly circular basin, so, when the periodic motion occurs extensively over the whole basin, the seiches may have almost the same period for all directions. The periodic motion in the N-S direction will be divided into two basins and the flow will be predominant in each basin, because the lake is almost symmetric as shown in Fig. 23. Furthermore, it is supported by Nakamura and Honda (1911) with the model experiment in which the periodic motion in the N-S direction is individually occurred in two basins. This flow pattern is shown as C in Fig. 23. When the lake is divided into two basins in the model of T–2 as shown in Fig. 22, the estimated period in the west basin is 9.2 min and that in the east basin is 9.1 min. They are almost equal to the observed one.

As a result, if outlines of a lake are almost the same no matter what the rectangular models of the lake differ in the length and the width each other, it may be concluded that their periods will almost coincide.

In natural lakes, the seiche periods were estimated in this way. The relation between the estimated and the observed periods are shown in Fig. 24. The left side diagram in this figure shows shorter periods (under 35

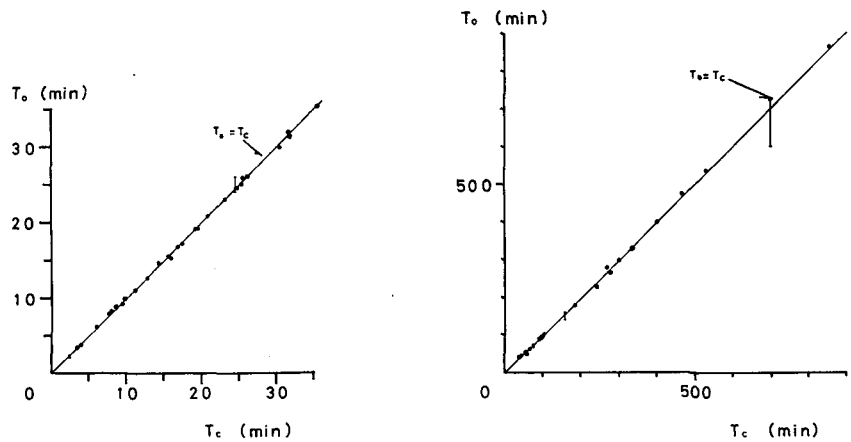

Fig. 24 Comparison of the estimated period (T_c) with the observed one (T_0) in the natural lake. The values are shown in Table 4.

Table 4 The estimated and the observed seiche periods in natural lakes.

Lake	Observed period (min)	Authors	L (km)	Estimated period (min)
Ammersee	24	Endrös (1934)	15.1	24.2
Aoki-ko	3.745	Tanaka (1930)	1.8	3.8
Ashi-no-ko	15.38	Nakamura and Honda (1911)	6.4	16.0
Lake Baikal	280	Sudol'skiy (1975)	590	270
Lake Balaton	600～720	Cholnoky (1897)*	76.6	697
Biwa-ko	229.8	Imasato et al. (1973)	57.3	246
Lake Brienz	9.8	Sarasin (1895)*	13.5	9.8
Chiemsee	41	Endrös (1906a)	14.0	40.8
Chuzenji-ko	7.77	Nakamura and Honda (1911)	6.8	7.6
Lake Constance	55.8	Forel (1893)*	46.7	55.5
Loch Earn	14.52	Chrystal (1908)*	10.5	14.4
Lake Erie	863	Platzman and Rao (1964)	376	852
Lago di Garda	42.92	Defant (1908)	52.2	42.5
Lake Geneva	73.5～74.2	Bircher (1954)**	65.2	73.7
Goldberger See	24～26	Klinker and Karbaum (1966)	3.9	24.5
Great Bear Lake	330	Johnson (1975)	272	330
Green Lake	26.0	Stewart (1964)	12.1	26.2
Lake Huron	400	Mortimer and Fee (1976)	330	399
Inawashiro-ko	19.11	Honda et al. (1911/1912)	13.8	19.1
Kasumi-ga-ura	140～160	Shio (1977)	29.0	156
Kawaguchi-ko	22.98	Nakamura and Honda (1911)	5.2	23.2
Kizaki-ko	6.117	Tanaka (1930)	2.42	6.0
Kutcharo-ko	30	Kodomari (1975)	12.4	30.3
Kuttara-ko	2.0～2.4	Tanakadate (1925)	2.45	2.5
Lake Lappajärvi	93	Simojoki (1961)	22.2	90.6
Madüsee	35.5	Halbfass (1902, 1903)*	15.3	35.5
Lake Mendota	25.8	Bryson and Kuhn (1952)	8.0	25.9
Lake Michigan	538	Mortimer and Fee (1976)	475	530
Lough Neagh	96	Darbyshire and Darbyshire (1957)	30.0	95.4
Loch Ness	31.5	Chrystal (1910)*	35.5	31.6
Nojiri-ko	8.9	Tanaka (1926)	3.2	8.6
Lake Ontario	300	Rao and Schwab (1976)	279	300
Lake Pyhäjärvi	101	Simojoki (1961)	25.1	101
Shikotsu-ko	8.05	Kusakabe et al. (1917)	12.2	7.8
Starnberger See	25	Ebert (1900)	19.0	25.2
St. Wolfgang See	32	Endrös (1906b)	10.7	31.6
Lake Superior	474	Mortimer and Fee (1976)	567	473
Suwa-ko	20.8	Tanaka (1911)	4.6	20.8
Lake Tahoe	19.0	Fee and Bachmann (1968)	36.4	19.2
Lake Tanganyika	270	Servais (1957)***	610	275
Tazawa-ko	3.5	Honda (1915)	6.4	3.6
Towada-ko	17.33	Honda et al. (1913)	9.4	17.4
Toya-ko	11.0	Kodomari (1978)	10.9	11.2
Loch Treig	9.18	Chrystal (1910)*	7.9	9.4
Lake Vetter	178.99	Bergsten (1926)	118.9	180
Waginger-Tachinger-Sees	62		9.4	61.3
(Waginger-See	16.8	Endrös (1905)	5.7	16.9)
(Tachinger-See	12.56		3.4	12.6)
Lake Wakatipu	52.0	Heath (1975)	55.0	53.6
Yamanaka-ko	15.61	Nakamura and Honda (1911)	4.75	15.6

* According to Hutchinson (1957) ** According to Mortimer (1979)
*** According to Defant (1961)

min), and the right side one shows longer periods. The estimated values coincide well with the observed ones. Their values are shown in Table 4. The length (L) in this table is that of a fitted lake model, so it does not necessarily coincide with the length of the longitudinal lake axis.

4. Flow characteristics of the periodic motion

4.1 Flow pattern

Fig. 25 shows the lake model in which a rectangular peninsula sites in the central region. The depth has a constant value of 10 m in each model. The water flows mainly from the east to the west arround the peninsula in the lower case. In the upper case, the water flows mainly from the south (or the north) to the north (or the south) in the half basin divided by the peninsula. Generally, a large peninsula will divide a lake into two basins, and the flow will occur in each basin.

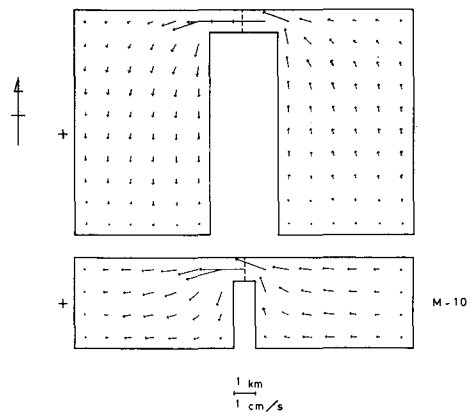

Fig. 25 Flow patterns in lakes (I). Broken line indicates the nodal line, and arrow shows the velocity vector.

Other flow patterns are numerically calculated as shown in Fig. 26. These lake models are supposed the constant depth of 10 m and the peninsula at the corner. In the case of the triangular peninsula, the water flows more smoothly than the case of the rectangular one.

Fig. 27 shows flow patterns at the time interval of five minutes in a lake model with the constant depth of 10 m. In this case, the water moves back and forth along the basin shape between two opposite lake shores. In the

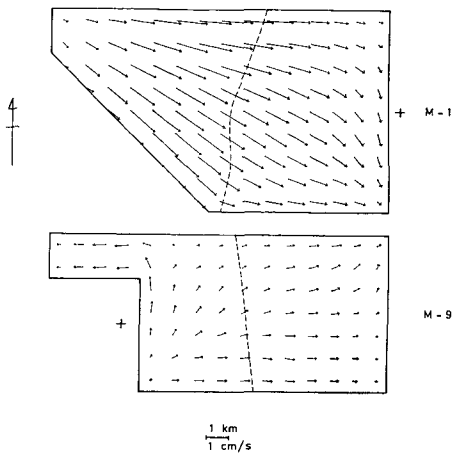

Fig. 26 Flow patterns in lakes (II).

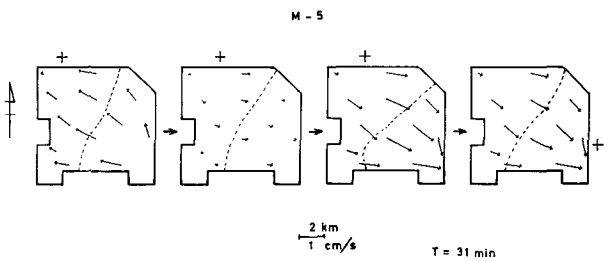

Fig. 27 Flow patterns in lakes (III). Flow patterns at the time interval of five minutes (in the model M–5). T is the period of the uninodal seiche.

case of a lake in which the bottom floor is uneven as shown in Fig. 28, the water moves back and forth in the central region of the lake, but at the longshore region it flows to only one direction each time step. In other words, the periodic motion in a natural lake may move not only back and forth, but also in one direction along the shore. As an example, calculated numerically (case Y–6 in Fig. 2), the water in the central region flows to the opposite direction of the longshore regions in Lake Yamanaka as shown in Fig. 29.

As described above, the water flows parallel to the lake basin shape, so stream lines in natural lakes may be estimated as follows: The fitted lake model is chosen, comparing the period estimated by the general formulas to the observed one. Consequently, stream lines are drawn parallel to the lake

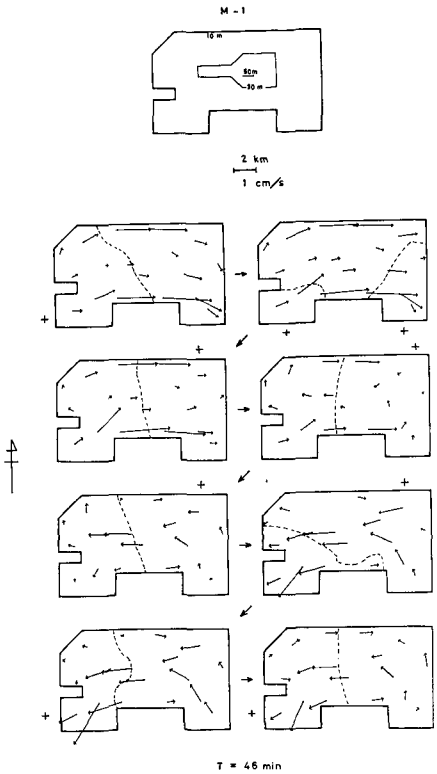

←Fig. 28 Flow patterns in lakes (IV). Flow patterns at the time interval of five minutes (in the model M–1). Upper figure indicates the deep area in the lake.

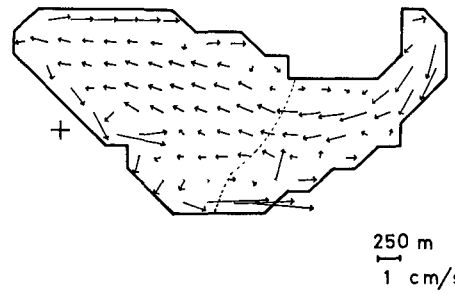

Fig. 29 Flow patterns in lakes (V). Case of the numerical calculation in Lake Yamanaka (case Y–6 in Fig. 2).

shore of this model. Because the periodic motion moves back and forth in the central region of the lake, moreover the flow direction is dependent on the direction of a given external force, the direction of the stream lines can not be determined. Figs. 30 and 31 show examples. Fig. 30 shows the estimated stream lines and the flow pattern which was numerically calculated in Lake Suwa (case S–3 in Fig. 1). The stream lines approximately agree with the flow pattern. Fig. 31 shows stream lines in Lake Nojiri, Nagano Prefecture in Japan. N-A and N-B are the cases estimated from the fitted lake models, and the stream lines in (A) and (B) were obtained with the model experiments by Tanaka (1926). The stream lines in N-A and N-B correspond to (A) and (B) respectively. These stream lines show very similar patterns. The period in the case of N-A is 8.6 min, in N-B is 6.7 min, in (A) is 8.81 min, and in (B) is 6.13 min. The observed periods are 8.9 and 6.5 min (Tanaka, 1926). They coincide well respectively.

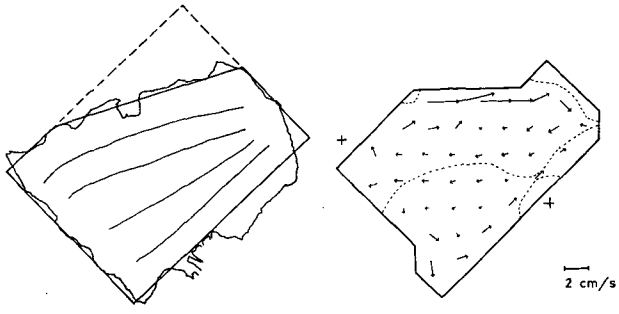

Fig. 30 Flow patterns in lakes (VI). Case in Lake Suwa. Left: stream lines estimated from the fitted lake model, Right: flow pattern obtained by the numerical calculation (case S–3 in Fig. 1).

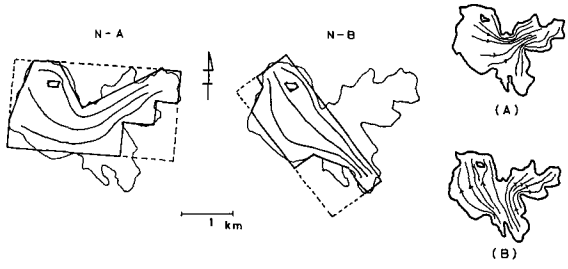

Fig. 31 Flow patterns in lakes (VII). Case in Lake Nojiri. N-A and N-B: stream lines estimated from the fitted lake models, (A) and (B): stream lines obtained by the model experiments (After Tanaka, 1926).

It is concluded that the estimated models give some information not only about the periods, but also about the flow patterns in natural lakes.

4.2 Position of the nodal line

As shown in Fig. 28, the position of the nodal line moves counterclockwise through each time step. This phenomenon had already been pointed out in some large lakes (e.g. Defant, 1953; Hamblin, 1976; Rao and Schwab, 1976).

The phase distribution of water level changes, calculated numerically, is shown in Fig. 32 by the solid lines in increments of 45°. The phase lines converge into the central part of the lake, so the distribution pattern of these phase lines is similar to the case having one nodal line. The fluctuation of water level at the central region is so small that the site of the nodal line is hardly found.

From these results, it can be considered that the nodal line locates itself about the fixed region.

Fig. 33 shows a schematic lake model. In this figure, L is the lake length, and x is the distance between the nodal line and the lake shore. Here, ΔT_R denotes a period increment affected by the right side geometry of the lake, and ΔT_L denotes an increment affected by the left side geometry. Being analogized from the balance, an equation for the position of the nodal line is given in the following,

$$\frac{L-x}{x} = \frac{T_0/2+\Delta T_R}{T_0/2+\Delta T_L} \ (\equiv A)\,,$$

then

$$x = \frac{L}{1+A}\,. \tag{26}$$

This equation was applied to the model case as shown in Fig. 32. In Fig. 34, the broken line shows the estimated nodal line, and its position coincides with the model case.

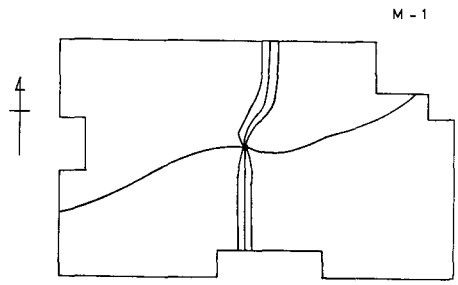

Fig. 32 Calculated structure of the first mode for a lake model (in the model M–1). Phase progression is shown by solid lines (45° intervals).

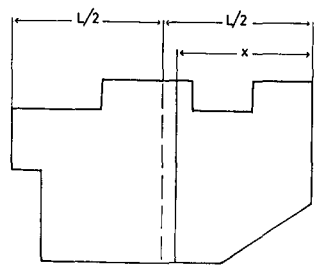

Fig. 33 Schematic model of the lake. Broken line shows the center line of the lake, and solid line shows the nodal line.

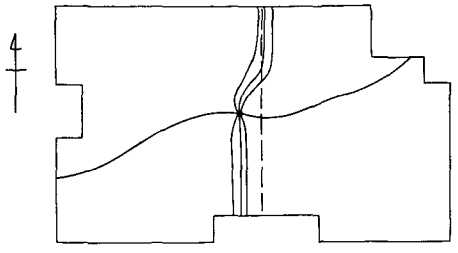

Fig. 34 Position of the nodal line (I). Broken line shows the estimated nodal line, and solid lines show the same lines as shown in Fig. 32.

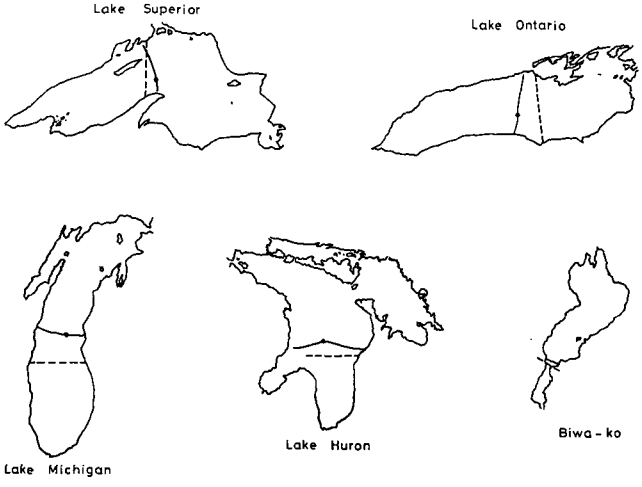

Fig. 35 Position of the nodal line (II). Solid line shows the nodal line obtained by the numerical calculation, and broken line shows that estimated using the equation (26).

Applying to natural lakes, the results are shown in Figs. 35, 36, and 37. In these figures, the different reduced scale is used on each lake. The nodal lines obtained by the numerical calculations and the equation (26) are shown in Fig. 35. In these cases, the numerical calculations using the two-dimensional models were performed in Lake Biwa by Imasato (1971), in Lake Michigan by Rao et al. (1976), in Lakes Ontario and Superior by Rao and Schwab (1976), and in Lake Huron by Schwab and Rao (1977). The nodal lines estimated by the equation (26) approximately agree with the numerically calculated ones in Lakes Huron, Superior, and Biwa, while those

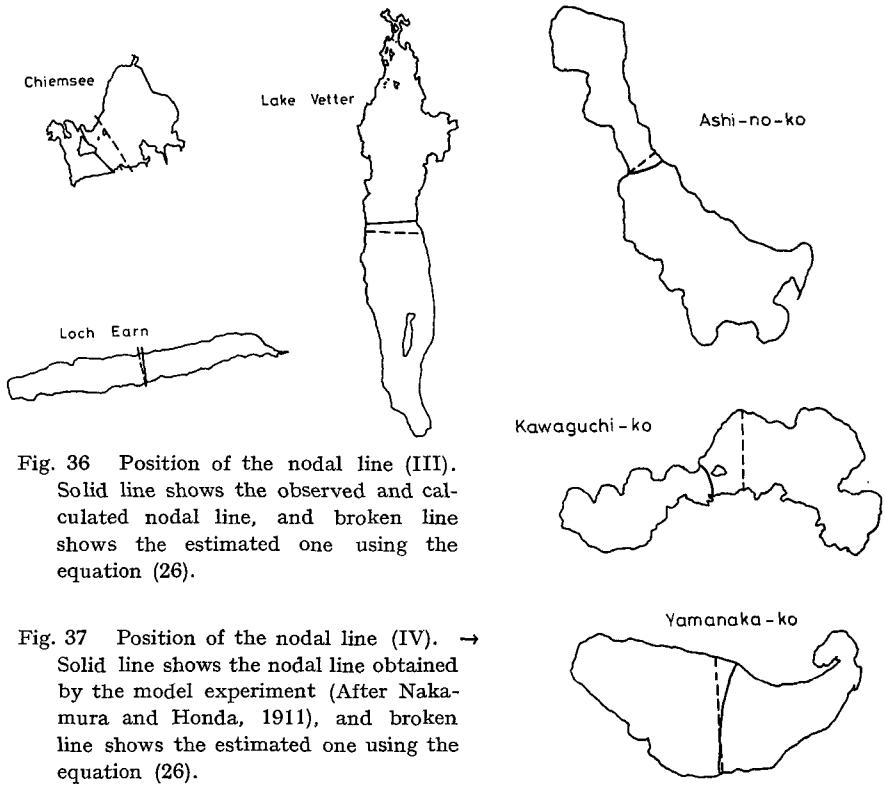

Fig. 36 Position of the nodal line (III). Solid line shows the observed and calculated nodal line, and broken line shows the estimated one using the equation (26).

Fig. 37 Position of the nodal line (IV). → Solid line shows the nodal line obtained by the model experiment (After Nakamura and Honda, 1911), and broken line shows the estimated one using the equation (26).

separate mutually at a short distance in the others. Fig. 36 shows the observed and calculated nodal line (solid line) and the estimated one (broken line). The calculations and the observations were done in Loch Earn by Chrystal and Wedderburn (1905), in Chiemsee by Endrös (1906a), and in Lake Vetter by Bergsten (1926). Two nodal lines coincide in Loch Earn, and they slightly differ in Lake Vetter, but they separate at a short distance in Chiemsee. Fig. 37 shows the nodal lines obtained from model experiments (solid line) and those estimated by the equation (26) (broken line). The model experiments were made by Nakamura and Honda (1911). Two nodal lines coincide in Lakes Yamanaka and Ashi-no-ko, Kanagawa Prefecture in Japan, but they separate at a short distance in Lake Kawaguchi, Yamanashi Prefecture in Japan.

As described in section *3.5*, fitted lake models have almost the same period in spite of the different rectangular models. The nodal lines in these

cases will be examined. In Lake Kutcharo, the nodal lines estimated by the equation (26) are shown in Fig. 38, according to the cases of K–1 and K–2 shown in Fig. 21. The solid circle indicates the observation point of water level, the fluctuation of the uninodal seiche could not observed at this point (Ko-

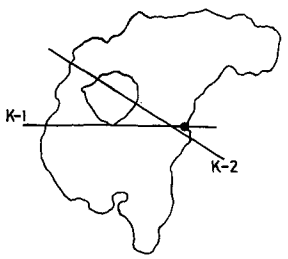

Fig. 38 Position of the nodal line (V). Case in Lake Kutcharo. K–1 and K–2 correspond to the cases as shown in Fig. 21. Solid circle shows the observation point of water level.

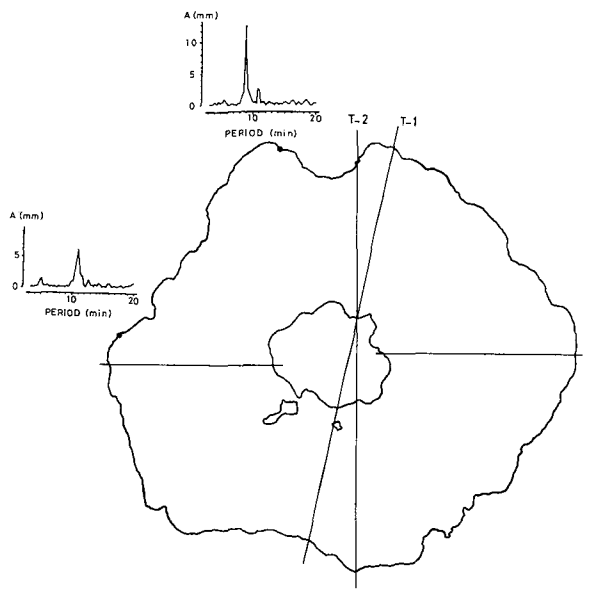

Fig. 39 Position of the nodal line (VI). Case in Lake Toya. T–1 and T–2 correspond to the cases in Fig. 22, and the other solid lines are the nodal lines for the transverse seiche in the model of T–2. Solid circles show the observation points of water level. The amplitude spectra at these points are shown (After Kodomari, 1978).

domari, 1975). Both the nodal lines exist at just position. The case of Lake Toya is shown in Fig. 39, the observation points of water level and the amplitude spectra at these points are shown (after Kodomari, 1978). The predominant period at the west shore is 11.0 min, while this at the north shore is 9.0 min. On the other hand, the period of 9.0 min is hardly seen at the west shore, and the period of 11.0 min is slightly found at the north shore. Because the observation points exist near the nodal lines, the periods according to the motions having these nodal lines are not confirmed at these points. Therefore, the estimated nodal lines in the cases of T–1 and T–2 locate themselves about good positions.

From the facts described above, it is concluded that the positions of the nodal lines can be estimated using the equation (26) in various lakes.

5. Effect of the Coriolis force

The Coriolis force deflects a flow direction to the right in the Northern Hemisphere and to the left in the Southern Hemisphere, looking in the direction of propagation. Therefore, the Coriolis force may act to deflect the flow of the periodic motion.

Generally, to consider the effect of the Coriolis force on the water motion, the Rossby number (R) is evaluated. It is defined in the following,

$$R = \frac{U}{fL}, \tag{27}$$

where U is the velocity of water, f is the Coriolis parameter, and L is the length of the motion.

For the special case of $R \ll 1$, the Coriolis force considerably affects the water motion. When the values are taken in the following, $U=1$ m/sec and $f=0.0001$/sec, a lake needs the length more than a few hundred kilometers to satisfy the condition of $R \ll 1$. This condition is satisfied only in some large lakes in the world. Several investigators have considered the effect of the Coriolis force in the Great Lakes (e.g. Platzman and Rao, 1964; Rao and Schwab, 1976; Schwab and Rao, 1977). They have concluded that the earth's rotation usually caused small increase in the seiche period of only the lowest mode, and the increment of the period was smaller than 1%. As a result, the effect of the Coriolis force on the seiche period is negligibly small in the natural lake.

Two model lakes with the constant depth of 10 m are shown in Fig. 40

(in the model M–5), where the left side figures ((A)) show the cases of no Coriolis force and the right side ((B)) show the flow patterns considering the Coriolis force. These flow patterns of (A) are nearly equal to those of (B), but the position of the nodal line is slightly different from each other. Because the island and the peninsula deflect the flow direction, the effect of the Coriolis force on the flow pattern is apparently negligibly small.

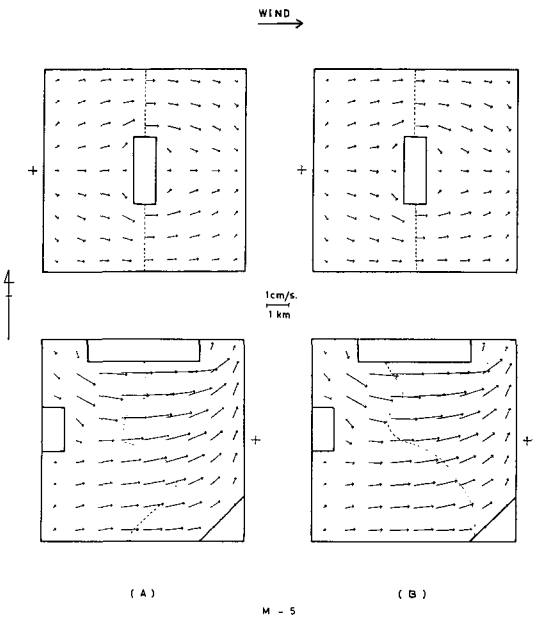

Fig. 40 Flow patterns in lakes (VIII). The effect of the earth's rotation on the flow pattern (in the model M–5). (A): the case of no Coriolis force, (B): the case considering the Coriolis force.

Excluding the Coriolis force, the numerical calculation was carried out in the same lake model as shown in Fig. 32. The calculated nodal line is shown in Fig. 41. In this model, the uninodal seiche has standing nature with a nodal line which is fixed in space all the time, but the position of it is nearly equal to the case considering this force as shown in Fig. 32. Namely, though the Coriolis force makes the nodal line to move with an amphidromic point, the phase lines converge into the nodal line in the case of no Coriolis force. When it is considered the position of the nodal line to fix, there is little difference between the case including the Coriolis froce and that excluding this force. For examples, the differences are little in Lakes Ontario, Superior (Rao

and Schwab, 1976), and Michigan (Rao et al., 1976). From the facts described above, the effect of the Coriolis froce on the position of the nodal line is negligibly small in appearance.

Consequently, it is concluded that the flow of the periodic motion generally depends only on the lake basin shape, because the effect of the Coriolis force is negligibly small. In other words, to investigate the periodic motion, it is sufficient to consider mainly the effect of the lake basin shape.

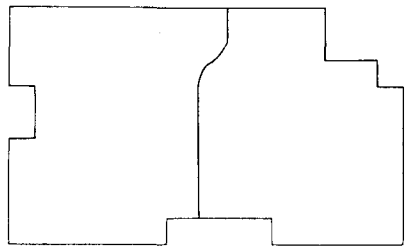

Fig. 41 Position of the nodal line (VII). The case of no Coriolis force. The lake model is the same as the case in Fig. 32.

6. Conclusions

The periodic motion in a lake was systematically considered, using the numerical calculations in typical lake models. As a result of investigating lots of models and comparing to the observations, it is concluded as follows:

(1) The general formulas to evaluate the effect of the lake basin shape on the period are obtained, and they are successful for various instances.

(2) Comparing the periods estimated by these formulas to the observed ones in natural lakes, the characteristics of the lake basin shape effect became evident systematically for the periodic motion of lake water.

(3) Generally, the effect of the lake basin shape including the existence of islands prolongs the seiche period than that calculated in the rectangular lake shape, but the effect of the bottom topography shortens that than that calculated using the mean depth. The reasons are considered as follows: The lake water is turned the flow direction by the existence of islands or peninsulas, it becomes sometimes dead water so that stagnates in an embayment region and becomes sometimes reverse flow in a cove. These flow patterns prolong the seiche period. The lake water below the mean depth affects the seiche period, and the effect generally acts to shorten it.

(4) The effect of the bottom topography can be evaluated considering the

increment of the depth, and the increment values are about 5~15% of the mean depths in natural lakes.

(5) Comparing the estimated period to the observed one, the flow pattern in a lake can be estimated. The stream lines can be drawn parallel to the lake basin shape in the fitted lake model. When the estimated flow patterns are compared to those obtained by the numerical calculations and the model experiments, they coincide well as shown in Figs. 30 and 31.

(6) The position of the nodal line changes unsteadily with time. However, these positions are at almost the same place and can be determined by the general formula of (26). The estimated positions approximately agree with the observations and the experimental studies by many investigators.

(7) The effect of the Coriolis force on the seiche period and the flow pattern is negligibly small in the natural lake. Therefore, the periodic motion is generally controlled by the lake basin shape.

(8) Finally, the seiche in a lake is not such a simple reciprocating motion as having been treated for calculations, but is the periodic motion with the complex flow pattern affected by the lake basin shape.

Acknowledgements

The author is grateful to Professor K. Nakao, Faculty of Science, Hokkaido University, for valuable discussions.

The numerical calculations in this article were carried out on FACOM 230-75 and HITAC M-180 in the Hokkaido University Computing Center. This paper is the author's doctorial thesis submitted to Hokkaido University in March, 1981.

References

Bergsten, F., 1926. The seiches of Lake Vetter, Geogr. Ann., **8**, 1–73.

Bryson, R.A. and P.M. Kuhn, 1952. On certain oscillatory motions of lakes, Report to the Univ. Wisconsin Lake Invest. Comm., No. 5, 9 pp.

Chrystal, G., 1904. Some results in the mathematical theory of seiches, Proc. Roy. Soc. Edinb., **25**, 328–337.

Chrystal, G., 1905a. Some further results in the mathematical theory of seiches, Proc. Roy. Soc. Edinb., **25**, 637–647.

Chrystal, G., 1905b. On the hydrodynamical theory of seiches. With a bibliographical sketch, Trans. Roy. Soc. Edinb., **41**, 599–649.

Chrystal, G. and E.M. Wedderburn, 1905. Calculation of the periods and nodes of Lochs Earn and Treig, from the bathymetric data of the Scottish Lake Survey, Trans. Roy. Soc. Edinb., **41**, 823–850.

Clarke, D.J., 1971. Seiche motions for a basin of rectangular plan and of nonuniform depth, J. Mar. Res., **29**, 47–59.

Darbyshire, J. and M. Darbyshire, 1957. Seiches in Lough Neagh, Quart. J.R. Met. Soc., **83**, 93–102.

Defant, A., 1908. Über die stehenden Seespiegelschwankungen (Seiches) in Riva am Gardasee, S.B. Akad. Wiss. Wien, Math. -Nat. Kl., **117**, *Abt IIa*, 697–780.

Defant, A., 1918. Neue Methode zur Ermittlung der Eigenschwingungen (Seiches) von abgeschlossenen Wassermassen (Seen, Buchten usw.), Ann. Hydr. Mar. Met., **46**, 78–85.

Defant, A., 1961. Physical Oceanography, vol. 2, Pergamon Press., 598 pp.

Defant, F., 1953. Theorie der Seiches des Michigansees und ihre Abwandlung durch Wirkung der Corioliskraft, Arch. Met. Geophys. Bioklimatol., **A6**, 218–241.

Ebert, H., 1900. Periodische Seespiegelschwankungen (Seiches), beobachtet am Starnberger See, S.B. bayer. Akad. Wiss., Math. -Phys. Kl., **30**, 435–462.

Einarsson, E. and A.B. Lowe, 1968. Seiches and set-up on Lake Winnipeg, Limnol. Oceanogr., **13**, 257–271.

Endrös, A., 1905. Die Seiches des Waginger-Tachingersees, S.B. bayer. Akad. Wiss., Math. -Phys. Kl., **35**, 447–476.

Endrös, A., 1906a. Die Seeschwankungen (Seiches) des Chiemsee, S.B. bayer. Akad. Wiss., Math. -Phys. Kl., **36**, 297–350.

Endrös, A., 1906b. Seichesbeobachtungen an den größeren Seen des Salzkammergutes, Petermanns Mitt., **52**, 252–258.

Endrös, A., 1934. Beobachtungen über die Dämpfung der Seiches in Seen, Gerl. Beitr. Geophys., **41**, 130–148.

Ertel, H., 1933. Eine neue Methode zur Berechnung der Eigenschwingungen von Wassermassen in Seen unregelmäßiger Gestalt, S.B. preuss. Akad. Wiss., **24**, 746–750.

Fee, E.J. and R.W. Bachmann, 1968. An empirical study of the Defant method of seiche analysis, Limnol. Oceanogr., **13**, 665–669.

Hamblin, P.F., 1976. Seiches, circulation, and storm surges of an ice-free Lake Winnipeg, J. Fish. Res. Board Can., **33**, 2377–2391.

Heath, R.A., 1975. Surface oscillations of Lake Wakatipu, New Zealand, N.Z.J. Mar. Freshwater Res., **9**, 223–238.

Hidaka, K., 1932a. Tidal oscillations in a rectangular basin of variable depth. (Problems of water oscillations in various types of basins and canals – Part IV), Mem. Imp. Mar. Obs., **5**, 15–23.

Hidaka, K., 1932b. Tidal oscillations in a rectangular basin of variable depth (Second paper) (Problems of water oscillations in various types of basins and canals – Part VI), Geophys. Mag., **5**, 265–271.

Hidaka, K., 1936. Application of Ritz's variation method to the determination of seiches in a lake, Mem. Imp. Mar. Obs., **6**, 159–174.

Hidaka, K., 1937. Tidal oscillations in a rectangular basin of variable depth (3rd paper) (Problems of water oscillations in various types of basins and canals – Part XI), Mem. Imp. Mar. Obs., **6**, 259–278.

Honda, K., 1915. On the ordinary and internal seiches in Lake Tasawa, Sci. Rep. Tohoku Imp. Univ., Ser. 1, **4**, 33–42.

Honda, K., K. Aichi, J. Okubo, Y. Yamashita, S. Sasaki, Y. Ogura, S. Mashima, S. Sato and H. Nagaoka, 1911/1912. On the seiches of Lake Inawasiro, Sci. Rep. Tohoku Imp. Univ., Ser. 1, **1**, 243–249.

Honda, K., J. Okubo, T. Matsuda, Y. Yamashita, S. Sasaki and Y. Ogura, 1913. On the seiches of Lake Towada, Sci. Rep. Tohoku Imp. Univ., Ser. 1, **2**, 163–169.

Hutchinson, G.E., 1957. A Treatise on Limnology, vol. 1, Wiley, 1015 pp.
Imasato, N., 1971. Study of seiche in Lake Biwa-ko (II) — On a numerical experiment by nonlinear two-dimensional model —, Contr. Geophys. Inst. Kyoto Univ., **11**, 77–90.
Imasato, N., 1972. Study of seiche in Lake Biwa-ko (III) — Some results of numerical experiments by nonlinear two-dimensional model —, Contr. Geophys. Inst. Kyoto Univ., **12**, 63–75.
Imasato, N., K. Tanaka and H. Kunishi, 1973. Study of seiche in Lake Biwa-ko (IV) — Observation with a new portable long period water level gauge —, Contr. Geophys. Inst. Kyoto Univ., **13**, 65–72.
Jeffreys, H., 1925. The free oscillations of water in an elliptical lake, Proc. Lond. Math. Soc., Ser. 2, **23**, 455–476.
Johnson, L., 1975. Physical and chemical characteristics of Great Bear Lake, Northwest Territories, J. Fish. Res. Board Can., **32**, 1971–1987.
Kanari, S., 1974. On the study of numerical experiments of two layer Lake Biwa, Jap. J. Limnol., **35**, 1–17.
Klinker, L. and H. Karbaum, 1966. Die Eigenschwingungen des Goldberger Sees, Acta Hydrophysica, **10**, 133–161.
Kodomari, S., 1975. Observations of water level and numerical experiments in Lake Kutcharo (in Japanese), Geophys. Bull. Hokkaido Univ., **34**, 1–14.
Kodomari, S., 1976. On the studies of the periodic motions in a lake (I) (in Japanese), Jap. J. Limnol., **37**, 123–130.
Kodomari, S., 1978. Study of seiches in Lake Toya (in Japanese), Geophys. Bull. Hokkaido Univ., **37**, 1–8.
Kusakabe, S., H. Saegusa, T. Matsushita, S. Saito, R. Joya, Y. Notsuki and H. Iwokibe, 1917. Internal seiches and undulation of the discontinuous layers in Lake Shikotsu, Sci. Rep. Tohoku Imp. Univ., Ser. 1, **6**, 31–40.
Lamb, H., 1932. Hydrodynamics, 6th ed., Cambridge Univ. Press, 738 pp.
Mortimer, C.H., 1979. Strategies for coupling data collection and analysis with dynamic modelling of lake motions, in Hydrodynamics of Lakes (W.H. Graf and C.H. Mortimer edited), Elsvier Scientific Publishing Company, 183–222.
Mortimer, C.H. and E.J. Fee, 1976. Free surface oscillations and tides of Lakes Michigan and Superior, Phil. Trans. R. Soc. Lond., Ser. A, **281**, 1–61.
Nakamura, S. and K. Honda, 1911. Seiches in Some Lakes of Japan, Jour. College Sci., Imp. Univ. Tokyo, **28(5)**, 95 pp.
Neumann, G., 1944a. Die Impedanz mechanischer Schwingungssysteme und ihre Anwendung auf die Theorie der Seiches, Ann. Hydr. Mar. Met., **72**, 65–79.
Neumann, G., 1944b. Eine Methode zur Berechnung der Eigenperioden zusammengesetzter (gekoppelter) Seebeckensysteme, Ann. Hydr. Mar. Met, **72**, 193–205.
Platzman, G.W., 1972. Two-dimensional free oscillations in natural basins, J. Phys. Oceanog., **2**, 117–138.
Platzman, G.W. and D.B. Rao, 1964. The free oscillations of Lake Erie, in Studies on Oceanography (K. Yoshida edited), Univ. Tokyo Press, 359–382.
Proudman, J., 1915. Free and forced longitudinal tidal motion in a lake, Proc. Lond. Math. Soc., Ser. 2, **14**, 240–250.
Proudman, J., 1953. Dynamical Oceanography, Methuen & CO LTD, 409 pp.
Rao, D.B., C.H. Mortimer and D.J. Schwab, 1976. Surface normal modes of Lake Michigan: Calculations compared with spectra of observed water level fluctuations, J. Phys. Oceanog., **6**, 575–588.
Rao, D.B. and D.J. Schwab, 1976. Two dimensional normal modes in arbitrary enclosed

basins on a rotating earth: Application to Lakes Ontario and Superior, Phil. Trans. R. Soc. Lond., Ser. A, **281**, 63–96.

Schwab, D.J. and D.B. Rao, 1977. Gravitational oscillations of Lake Huron, Saginaw Bay, Georgian Bay, and the North Channel, J. Geophys. Res., **82**, 2105–2116.

Shio, K., 1977. Changes of water level in Kasumi-ga-ura (in Japanese), in Kasumi-ga-ura (Coll. Agriculture Ibaragi Univ. edited), Sankyo-Shuppan, 14–16.

Simojoki, H., 1961. On seiches in some lakes in Finland, Geophysica, **7**, 145–150.

Stewart, R., 1964. On the estimation of lake depth from the period of the seiche, Limnol. Oceanogr., **9**, 606–607.

Sudol'skiy, A.S., 1975. Distribution of wind-driven currents in bodies of water and estimation of the transport of water by them, Soviet Hydrology, Selected Papers, No. 3, 147–154.

Tanaka, A., 1911. On the seiches in Suwa Lake (in Japanese), Ryigaku-kai, **8**, 518–522.

Tanaka, A., 1926. Studies in Nojiri Lake (in Japanese), Kokonshoin, 636 pp.

Tanaka, A., 1930. Studies in Lakes of the North Japan Alps (in Japanese), Kokonshoin, 1036 pp.

Tanakadate, S., 1925. General Report of the Studies on the Volcanic Lakes in Hokkaido (in Japanese), Hokkaido Government, 155 pp.

Terada, T., 1906. Notes on seiches, Proc. Tokyo math. -phys. Soc., **3**, 174–181.

Tuboi, I., 1936. Free oscillations in a lake having non-elongated and smooth boundary, Mem. Imp. Mar. Obs., **6**, 227–237.